Neurochemistry International 129 (2019) 104494

Contents lists available at ScienceDirect

Neurochemistry International

journal homepage: www.elsevier.com/locate/neuint

Mechanical allodynia induced by optogenetic sensory nerve excitation activates dopamine signaling and metabolism in medial nucleus accumbens

Eiji Sugiyama[a], Takashige Kondo[b], Naoko Kuzumaki[b,c], Kurara Honda[a], Akihiro Yamanaka[d], Minoru Narita[b,c], Makoto Suematsu[a], Yuki Sugiura[a,*]

[a] Department of Biochemistry, Keio University School of Medicine, 35 Shinanomachi, Shinjuku, Tokyo, 160-8582, Japan
[b] Department of Pharmacology, Hoshi University School of Pharmacy and Pharmaceutical Sciences, Tokyo, Japan
[c] Life Science Tokyo Advanced Research Center (L-StaR), Hoshi University School of Pharmacy and Pharmaceutical Sciences, Tokyo, Japan
[d] Department of Neuroscience II, Research Institute of Environmental Medicine, Nagoya University, Nagoya, 464-8601, Japan

ARTICLE INFO

Keywords:
Dopamine
Nucleus accumbens
Ventral tegmental area
Mechanical allodynia
Optogenetics
Imaging mass spectrometry

ABSTRACT

The mesolimbic dopaminergic signaling, such as that originating from the ventral tegmental area (VTA) neurons in the medial part of the nucleus accumbens (mNAc), plays a role in complex sensory and affective components of pain. To date, we have demonstrated that optogenetic sensory nerve stimulation rapidly alters the dopamine (DA) content within the mNAc. However, the physiological role and biochemical processes underlying such rapid and regional dynamics of DA remain unclear. In this study, using imaging mass spectrometry (IMS), we observed that sensitized pain stimulation by optogenetic sensory nerve activation increased DA and 3-Methoxytyramine (3-MT; a post-synaptic metabolite obtained following DA degradation) in the mNAc of the experimental mice. To delineate the mechanism associated with elevation of DA and 3-MT, the *de novo* synthesized DA in the VTA/substantia nigra terminal areas was evaluated using IMS by visualizing the metabolic conversion of stable isotope-labeled tyrosine ($^{13}C^{15}N$-Tyr) to DA. Our approach revealed that at steady state, the *de novo* synthesized DA occupied > 10% of the non-labeled DA pool in the NAc within 1.5 h of isotope-labeled Tyr administration, despite no significant increase following pain stimulation. These results suggested that sensitized pain triggered an increase in the release and postsynaptic intake of DA in the mNAc, followed by its degradation, and likely delayed *de novo* DA synthesis. In conclusion, we demonstrated that short, peripheral nerve excitation with mechanical stimulation accelerates the mNAc-specific DA signaling and metabolism which might be associated with the development of mechanical allodynia.

1. Introduction

The dopaminergic pathway, present from the ventral tegmental area (VTA) to the nucleus accumbens (NAc), is important for mediating acute and chronic pain sensations (Ikemoto, 2007; Taylor et al., 2016) and pain-avoidance behavior (Danjo et al., 2014). The medial part of the NAc (mNAc) integrates signals from the mesencephalic dopaminergic neurons and other brain areas that process affective information (Britt et al., 2012; Bromberg-Martin et al., 2010). Recent studies have shown that one projection of the mNAc, the indirect pathway (Bromberg-Martin et al., 2010), is associated with the affective evaluation of events that shape behavior *via* interaction of dopamine (DA) with the D2 receptors (Ren et al., 2016). This pathway participates in the central representation of pain, and controls the activity of the ascending nociceptive pathways (Ren et al., 2016).

Accumulating evidence show that input from the VTA neurons, *via* DA signaling in the mNAc, plays a key role in the indirect pathway. We recently reported that activation of dopaminergic neurons in the VTA increases the amount of extracellular DA within the NAc, which blunts pathological allodynia induced by nerve injury or bone cancer (Watanabe et al., 2018a). Moreover, manipulating the excitability of mNAc by administering a DA agonist diminishes mechanical allodynia in spared nerve injury models of neuropathic pain (Sarkis et al., 2011). In contrast, aversive stimuli inhibit the dopaminergic neurons of the VTA (Danjo et al., 2014; Moriya et al., 2018; Ungless et al., 2004).

To disentangle the complex sensory and affective components of pain, optogenetic manipulation of sciatic nerve neurons has been used to induce noninvasive excitation of nociceptors in freely moving mice (Iyer et al., 2014). Using this method, we observed that exclusive excitation of the sciatic nerves by blue light lowered the pain threshold

* Corresponding author.
E-mail address: yuki.sgi@keio.jp (Y. Sugiura).

https://doi.org/10.1016/j.neuint.2019.104494
Received 19 December 2018; Received in revised form 12 June 2019; Accepted 21 June 2019
Available online 21 June 2019

but did not induce pain sensation, and was accompanied by a mNAc-specific reduction of DA as measured by imaging mass spectrometry (IMS) (Watanabe et al., 2018b). IMS measures the biochemical content (Morikawa et al., 2012), for example, the total amount of DA from each pixel in tissue sections (Shariatgorji et al., 2014); therefore, our observation indicated rapid and large fluctuations in the total amount of DA, most likely, manifested by the stored synaptic vesicular pool of DA at mNAc-nerve terminals, which may be associated with the reduced pain threshold. However, it remains unclear whether sensitized pain stimulation by optogenetic nerve excitation alters the regional DA content. Moreover, the biochemical processes mediating the fluctuation of DA need to be elucidated.

In this study, we approached this question by visualizing the regional DA content, as well as the metabolic conversion of stable isotope-labeled Tyr ($^{13}C^{15}N$-Tyr) to DA ($^{13}C^{15}N$-DA), using IMS. The amount of non-labeled DA and *de novo* synthesized $^{13}C^{15}N$-DA from the exogenously administrated $^{13}C^{15}N$-Tyr was evaluated within the caudate putamen (CP), mNAc, lateral part of the nucleus accumbens (lNAc), and VTA. Using this technique, we demonstrate if mechanical allodynia induced by optogenetic sensory nerve excitation activates medial mNAc-specific dopamine signaling and metabolism.

2. Material and methods

2.1. Mice

Male C57BL/6J mice (8–12 weeks old; Tokyo Laboratory Animals Science Co., Ltd., Tokyo, Japan) were housed (up to six per cage) and maintained in a temperature-controlled room (24 ± 1 °C). All mice were maintained under a 12-h light–dark cycle (light was switched on at 8 a.m.), and behavioral tests were performed during the light phase. Food and water were provided *ad libitum*. All animal experiments were performed in accordance with the Guiding Principles for the Care and Use of Laboratory Animals, Hoshi University, as adopted by the Committee on Animal Research of Hoshi University.

2.2. Time course analysis of dopamine de novo synthesis

After 12–15 h of food deprivation, the mice received oral administration of $^{13}C_9{}^{15}N_1$-Tyrosine ($^{13}C^{15}N$-Tyr; Taiyo Nippon Sanso, Tokyo, Japan; 30 mg/mL in H_2O, 10 μL/g body weight). After 0.5, 1.0, and 1.5 h, the mice were sacrificed and their brains were harvested and immediately flash frozen in solid CO_2 and stored at −80 °C.

2.3. Activation of sensory neurons by blue light irradiation

Based on the protocol described by Iyer et al., we used an adeno-associated virus serotype 6 (AAV6) encoding the human synapsin 1 promoter to achieve neuron-specific expression of the blue light–-sensitive cation channel, channelrhodopsin-2 (ChR2), (ET/TC) fused to enhanced yellow fluorescent protein (EYFP). The AAV6-hSyn-ChR2 (ET/TC)-EYFP or control AAV6-hSyn-EYFP were serotyped with AAV6 coat proteins and packaged at the viral vector core at Nagoya University. The final viral concentration was between 1×10^{11} and 3×10^{12} copies/mL. Aliquots of the viral solution were stored at −80 °C until use.

To selectively express ChR2-EYFP or EYFP in the sensory nerves, AAV6-hSyn-ChR2 (ET/TC)-EYFP or control virus was microinjected into the sciatic nerve of C57BL/6J mice. Briefly, the mice were anesthetized under isoflurane (3%, inhalation) and a 2-cm incision was made to expose the sciatic nerve. The microinjection was performed with an internal cannula (Eicom, Kyoto, Japan) at a rate of 1 μL/min for 8 min using a gas-tight syringe (10 μL; Eicom) and pump (Model ESP-32; Eicom). Two weeks after the intrasciatic injection, following 16 h of food deprivation, the mice were orally administered with $^{13}C^{15}N$-Tyr. Mice received optical stimulation (473 nm, continuous wave [CW], 0.5 h) to the plantar surface of the ipsilateral hind paw, 1.5 h after $^{13}C^{15}N$-Tyr administration. Thirty minutes after the optical stimulation, the mice were sacrificed the whole brains harvested and flash frozen in solid CO_2 and stored at −80 °C.

2.4. Measurement of the sensitivity for tactile stimulus

To quantify the change in pain sensitivity to tactile stimulus induced by the optical activation of sensory nerves, the paw withdrawal response was measured, in response to a tactile stimulus during blue light stimulation (473 nm, CW) of the plantar surface, using von Frey filaments with a bending force of 0.16 g (AesthesioV R, DanMic Global, LLC, CA, USA). Each of the hind paws were tested individually. Paw withdrawal in response to tactile stimulus was evaluated by scoring as follows: 0, no response; 1, a slow and slight withdrawal response; 2, a slow and prolonged fiexion withdrawal response (sustained lifting of the paw) to the stimulus; 3, a quick withdrawal response away from the stimulus without flinching or licking, and 4, an intense withdrawal response away from the stimulus with brisk flinching and/or licking. Paw movements associated with locomotion or weight shifting were not considered as a response.

2.5. Imaging mass spectrometry

Thin sections (thickness, 8 μm) were cut with a cryomicrotome (CM3050, Leica Microsystems) and thaw-mounted on indium-tin-oxide-coated glass slides (Bruker Daltonics, MA, USA) at −16 °C. After sectioning, deuterium-labeled dopamine (D_4-DA; 5 μM in 50% MeOH; IsoSciences PA, USA), used as an internal standard, was spray-coated on the sections using a robotic sprayer device (SunCollect system, SunChrom, Friedrichsdorf, Germany). To perform on-tissue derivatization of monoamines (Shariatgorji et al., 2014), the sections were manually spray-coated with a solution of 2,4-diphenyl-pyranylium (DPP) tetrafluoroborate salts (Sigma-Aldrich, MO, USA; 1.3 mg/mL in methanol) using an artistic airbrush (Procon Boy FWA Platinum 0.2-mm caliber airbrush, Mr. Hobby, Tokyo, Japan). Thereafter, the sections were automatically spray-coated with 2,5-dihydroxybenzoic acid as a matrix (40 mg/mL, dissolved in 50% methanol) using a robotic sprayer.

Data were acquired with an orbitrap mass spectrometer (QExactive Focus, Thermo Fisher Scientific) coupled with an atmospheric pressure scanning microprobe matrix-assisted laser desorption/ionization ion source (AP-SMALDI10, TransMIT GmbH, Giessen, Germany) or a linear ion trap mass spectrometer with another MALDI source (LTQ XL, Thermo Fisher Scientific). The raster step size was set at 80 μm (Fig. 1), 120 μm (Fig. 2), or 100 μm (Figs. 3 and 4). For the orbitrap mass spectrometer, signals within a mass range between 350 and 400 were acquired with a mass resolving power of 70,000 at m/z 200. For the linear ion trap mass spectrometer, signals of DPP-DA (m/z 368 > 232), DPP-D_4-DA (m/z 372 > 232), and DPP-$^{13}C^{15}N$-DA (m/z 377 > 233) were monitored with a precursor ion isolation width of m/z 1.0. Thereafter, the spectral data were transformed to image data and analyzed using ImageQuest 1.0.1 (Thermo Fisher Scientific), SCiLS 2019a (Bruker Daltonics) and ImageJ 1.51 (National Institutes of Health, USA) software.

3. Results

3.1. Mapping in situ concentrations of DA within the VTA/SN circuits

DA mapping by IMS revealed that *in situ* DA concentrations were unevenly distributed within the VTA/SN neuronal circuits. Tyrosine hydroxylase (TH)-positive neural somas were localized to the VTA/substantia nigra (SN) regions; however, we found that DA was highly concentrated in CP and NAc terminal regions, with concentrations 10-fold higher than that in the SN and VTA (Fig. 1). This observation

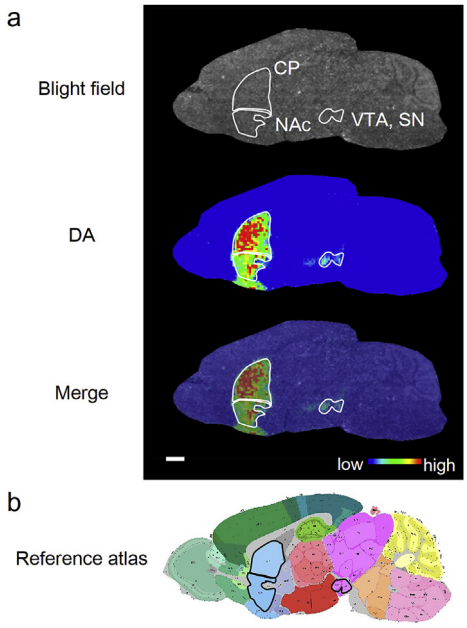

Fig. 1. Representative dopamine distribution in a sagittal slice of mouse brain. **a**. Representative image of a sagittal section of mouse brain imaged under bright field (top), IMS for DA (middle), and merged (bottom). Scale bar, 1 mm. **b**. Reference atlas (http://atlas.brain-map.org/) corresponding to the coordinates of the section shown in **a**. IMS, imaging mass spectrometry; CP, caudate-putamen; NAc, nucleus accumbens; VTA, ventral tegmental area; SN, substantia nigra.

indicated that local *de novo* synthesis of DA and/or rapid monoamine recycling at the CP and NAc synapses facilitated the accumulation of high levels of DA in the terminal areas.

3.2. In situ metabolic turnover analysis of DA synthesis

Following the observation of regional differences in DA concentration, we sought to assess the mechanism underlying the maintenance of high DA levels in the CP and NAc. To answer this, we evaluated the involvement of *de novo* synthesized DA in these terminal regions. Stable isotope-labeled Tyr ($^{13}C^{15}N$-Tyr) was orally administered to mice, and its conversion to *de novo* synthesized, labeled DA ($^{13}C^{15}N$-DA) was visualized in the brain sections comprising the CP and NAc at 0.5, 1.0, and 1.5 h after administration (Fig. 2a–c). The results revealed an unexpectedly fast replacement of the total DA pool with the *de novo* synthesized, labeled DA, within 1.5 h of $^{13}C^{15}N$-Tyr administration. The newly synthesized DA increasingly accumulated in the terminal area (Fig. 2c and d), and eventually, occupied > 10% of the non-labeled DA in the three terminal regions such as: CP, mNAc, and lNAc (Fig. 2e). In addition, an uneven rate of DA replacement between the brain regions was observed, with the mNAc exhibiting a lower replacement rate than that in the CP. These data indicate that a continuous and large supply of newly synthesized DA accumulates at the terminal regions to produce large storage pools of DA.

3.3. Sensitized pain stimulation during optogenetic sensory nerve activation increased regional levels of DA and 3-MT in mNAc

Since DA signaling in the NAc affects the pathological formation of allodynia (Watanabe et al., 2018a), subsequently, we hypothesized that sensitized pain sensation might accompany spatiotemporal DA fluctuation within the VTA/SN circuits. To verify this hypothesis, mice expressing ChR2-EYFP or EYFP were fed with $^{13}C^{15}N$-Tyr (Fig. 3a) and subjected to von Frey filament test for tactile stimulus during optogenetic stimulation with blue light irradiation. The results show a clear

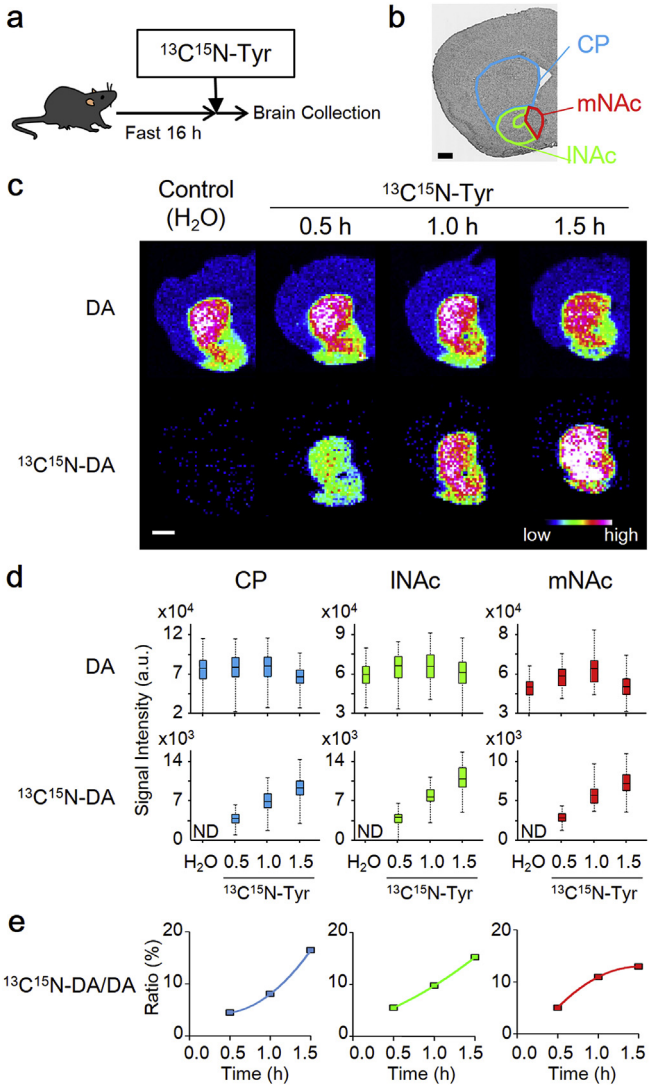

Fig. 2. Time course analysis of dopamine metabolic turnover with in the striatum. **a**. Experimental design. **b**. Representative image showing the striatal sub-regions. Scale bar, 0.5 mm. **c**. Ion images showing the levels of DA (upper) or $^{13}C^{15}N$-DA (lower). Scale bar, 1 mm. **d**. Box showing the signal intensities of DA (upper) or $^{13}C^{15}N$-DA (lower) at all pixels within striatal sub-regions. The three horizontal lines of the boxed section represents first, second, and third quartile from the bottom to top, respectively. Lines extending vertically from the boxes represent minimum and maximum. **e**. Mean $^{13}C^{15}N$-DA/DA ratio at each time point. DA, dopamine; CP, caudate-putamen; NAc, nucleus accumbens; lNAc, lateral part of the nucleus accumbens; mNAc, medial part of the nucleus accumbens.

elevation in allodynia score in mice expressing EYFP-ChR2 (Fig. 3b). Thereafter, their regional DA contents were visually examined in coronal sections at two positions within the CP/NAc and VTA, respectively (Fig. 3c, Supplementary Fig. 1). Interestingly, EYFP-ChR2 group exhibiting elevated allodynia score showed significantly higher DA content in the mNAc, than EYFP-group (Fig. 3d and e). This spatiotemporal increase in DA accompanied no significant increase in the *de novo* synthesized $^{13}C^{15}N$-DA.

Moreover, amount of 3-MT, a post-synaptic metabolite of DA degradation, increased over a wide area, including the CP, lNAc, and mNAc (Fig. 3d and e). These results suggest that tactile stimulation during blue light irradiation increased the release of DA, followed by its post-synaptic degradation to 3-MT, after which, the mNAc presumably received preferential supply (i.e., *de novo* synthesis and/or reuptake) of DA. Additionally, we found that the VTA showed a higher *de novo*

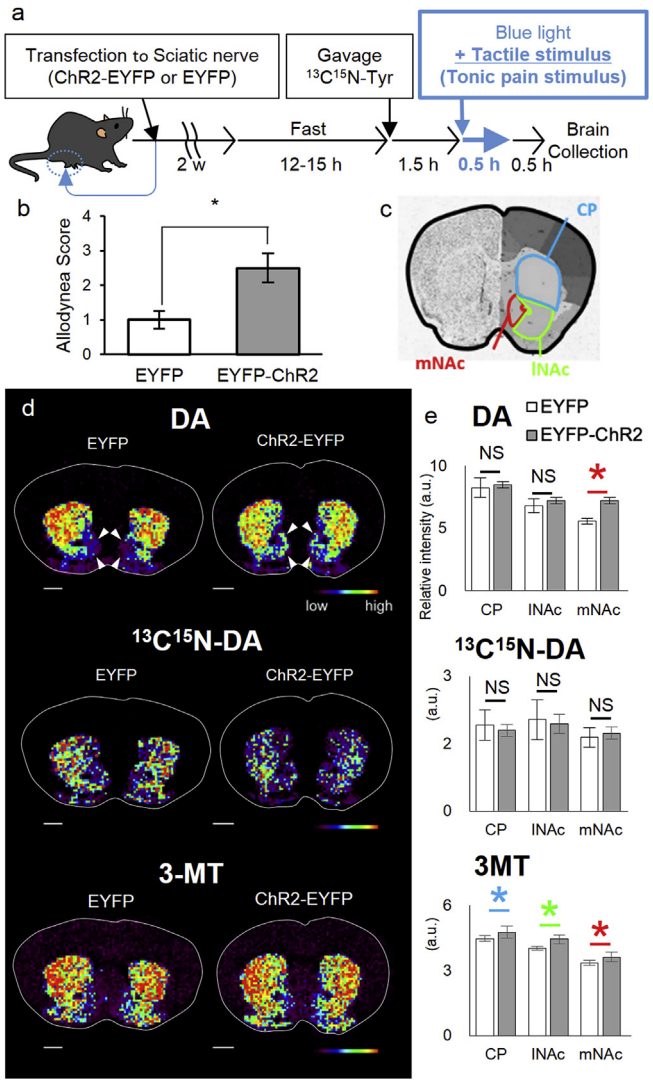

Fig. 3. Altered dopamine dynamics by optogenetic and tactile stimuli for the sciatic nerve. **a.** Experimental design. **b.** Effects of the optical activation of sensory nerves on the pain threshold. von Frey filaments were used to observe response to tactile stimulus during optical stimulation of the plantar surface. Data are presented as mean ± S.E. *: $p < 0.05$ (Welch's *t*-test). **c.** Reference atlas of the slices containing the target regions. The measured regions are enclosed within black lines. **d.** Representative ion images showing DA, $^{13}C^{15}N$-DA, and 3-MT in the striatum. White lines enclose the measured regions. White arrow heads indicates altered DA levels at mNAc. **e.** Mean levels of DA, $^{13}C^{15}N$-DA, and 3-MT in the striatum. Scale bar: 0.5 mm. Data are expressed as mean ± S.D. *$p < 0.05$ (Welch's *t*-test). DA, dopamine; 3-MT, 3-methoxytyramine; CP, the caudate-putamen; lNAc, lateral part of the nucleus accumbens; mNAc, medial part of the nucleus accumbens.

synthesized DA replacement rate than did the other three regions (Supplementary Fig. 1). These data indicate that the VTA has a higher activity of TH-driven DA synthesis and smaller pools of stored DA than that in the terminal regions.

3.4. Sciatic nerve excitation without tactile stimulation induced a reduction of DA in striatum but did not impair de novo DA synthesis

Optogenetic excitation of the sciatic nerve, without mechanical stimulation, induces aversion behavior in mice expressing ChR2-EYFP (Iyer et al., 2014); thus, we assessed the regional DA dynamics in mice under such condition. After the administration of stable isotope-labeled Tyr ($^{13}C^{15}N$-Tyr), brains were harvested from mice who received and

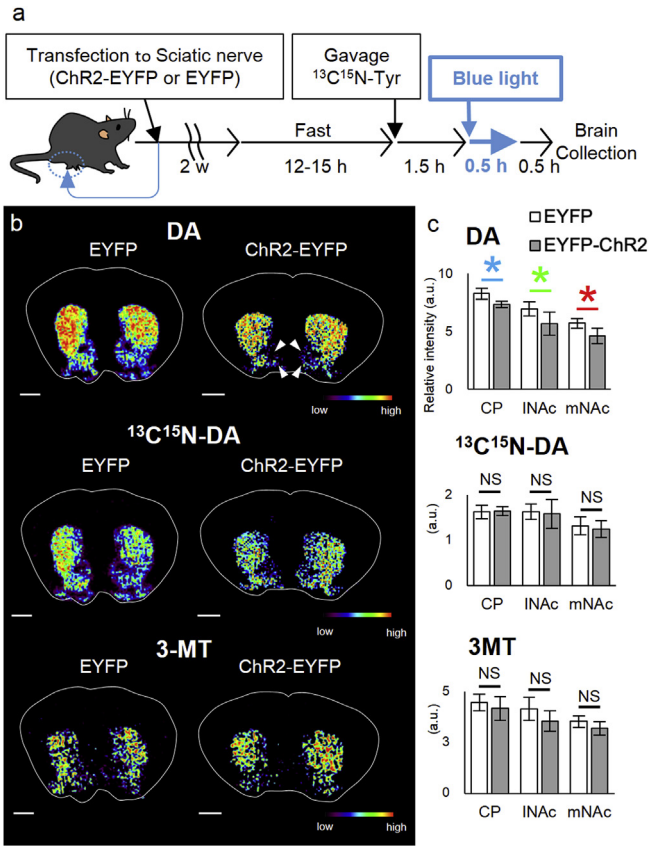

Fig. 4. Altered dopamine dynamics by optogenetic stimulation of the sciatic nerve. **a.** Experimental design. **b.** Representative ion images showing DA, $^{13}C^{15}N$-DA, and 3-MT. The upper section includes the striatum and the lower includes the VTA. White lines enclose the measured regions. White arrow heads indicates altered DA levels at mNAc. **c.** Mean levels of DA, $^{13}C^{15}N$-DA, and 3-MT in the striatum. Scale bar: 0.5 mm. Data are expressed as mean ± S.D. *: $p < 0.05$ (Welch's *t*-test). DA, dopamine; 3-MT, 3-methoxytyramine; CP, the caudate-putamen; lNAc, lateral part of the nucleus accumbens; mNAc, medial part of the nucleus accumbens.

did not receive blue light stimulation for 30 min (Fig. 4a). Interestingly, visualization by IMS demonstrated significant reduction of non-labeled DA in the CP and NAc terminal regions; however, no change was detected in the VTA (Fig. 4b and c, Supplementary Fig. 2). In contrast, the level of labeled DA remained unaltered in the CP and NAc, whereas slight reduction was observed in the VTA (Fig. 4c, Supplementary Fig. 2). Taken together, only those mice which received blue light stimulation without tactile stimulation showed reduced amount of DA in wide areas of the CP and NAc terminal regions, as well as suppressed *de novo* DA synthesis within the VTA.

4. Discussion

In this study, we demonstrated the presence of a high homeostatic level of DA in the striatum sub-regions, with a continuous supply of *de novo* synthesized DA. The *de novo* synthesized DA occupied a significant proportion of the non-labeled DA pool in the sub-regions within 1.5 h of $^{13}C^{15}N$-Tyr administration. Although our results are consistent with that of previous studies demonstrating fast DA turnover (Karoum et al., 1984; Kilts and Anderson, 1987), our technique provided spatially resolved information on the metabolic turnover of DA as high resolution images.

The DA levels visualized by IMS represent the sum of the intra- and extra-cellular DA concentration at any given pixel. Because the concentration of intracellular DA is typically much higher than

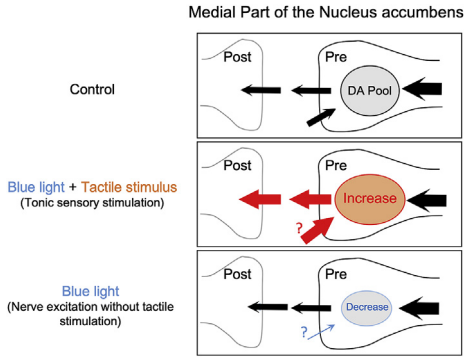

Fig. 5. Hypothesized model of altered dopamine dynamics in response to optogenetic stimulation with/without tactile stimulus on the sciatic nerve. Top: A model of DA dynamics in the medial part of the nucleus accumbens without any excess simulation. The majority of the DA is stored in synaptic vesicles at the pre-synapse. Wider horizontal lines indicate faster flow of DA. Middle: Optogenetic and tactile stimuli to the sciatic nerve, which cause pain-avoidance behavior, increase DA flow and the stored DA. Bottom: Optogenetic stimulus to the sciatic nerve, which causes decrease in pain threshold but not pain-avoidance behavior, decreases in DA flow, and stored DA.

extracellular DA (Ortiz et al., 2010), the DA dynamics observed in this study predominantly reflect changes in the intracellular DA concentration, most likely present in storage vesicle, localized at the nerve terminals (Kai-Kai, 1984). To overcome this technical challenge, we developed a micro-dialysis technique coupled with mass spectrometry (Watanabe et al., 2018b) to enable the comprehensive measurement of extra-cellular metabolites of DA degradation. Thus, the evaluation of vesicle-secreted DA and related metabolites, including stable isotope-labeled DA, by the microdialysis-mass spectrometry, is an important complementary approach for further study of DA metabolism.

Our IMS-based approach revealed elevated levels of DA and 3-MT in the NAc terminals following short-term tactile stimulus, sensitized by optogenetic excitation of the sciatic nerve. Thus, it is reasonable to state that DA metabolism, i.e., release and post-synaptic uptake followed by decomposition of DA, was activated during pain sensation, although the reuptake activity was not examined (Fig. 5). A recent report supports this suggestion; Mikhailova et al. showed that tail pinch treatment increased extra-cellular DA concentration in the NAc, whereas only touch stimulus did not alter the NAc DA concentration (Mikhailova et al., 2019). Other studies reported that pain stimuli, in addition to analgesia, increased the extra-cellular DA concentration in the NAc (Kato et al., 2016; Navratilova et al., 2015), suggesting that activated DA metabolism might be a feedback reaction to sensations of acute pain, and may play a role to attenuate the excess pain stimuli in the NAc.

On the contrary, in the striatum, optogenetic sensory nerve stimulation or tactile stimulus did not change the level of isotope-labeled DA (Fig. 4c). In contrast, a slight but significant decrease in isotope-labeled DA was observed in the VTA by optogenetic sensory nerve stimulation (Supplementary Fig. 2). These results suggest that DA production is more stable in the striatum than in the VTA. These observations may be congruent to reports which state that acute aversive stimuli induce a robust increase in extracellular DA level in the NAc but inhibits the firing of VTA DA neurons (Holly and Miczek, 2016; Ungless et al., 2004). An alternative interpretation of the unaffected *de novo* DA synthesis in mNAc is that such elevation of DA synthesis might be a slow process, and thus, the present results only show a marginal increase following optogenetic and tactile stimuli, which is statistically insignificant (Fig. 3e). In future studies, this hypothesis can be validated by assessing the *de novo* DA synthesis at a later time point from that of isotope-labeled Tyr administration. Nonetheless, large and stable local *de novo* DA synthesis within the terminal structures of the striatal nerve terminal is suggested to be a major source of DA, as opposed to its transportation from the VTA (Fibiger et al., 1973). In support of this suggestion, a previous study showed that restoration of DA synthesis in the striatal sub-regions, by region-specific TH expression alone, is sufficient, at least in part, to recover the affected behaviors in a DA deficient mouse model (Szczypka et al., 2001).

In summary, we show that the DA neurons in the mNAc increases the biochemical pool of DA in response to the short-term pain sensation. However, the detailed molecular mechanism and its pathophysiological significance remains unclear. Here, we only examined acute pain stimulation. On the contrary, Ren et al. (2016) reported that the basal extracellular DA level is decreased in the spared nerve injury model of chronic neuropathic pain. In addition, a single, acute stress promotes long-lasting neuroplastic changes in the VTA dopaminergic neurons (Graziane et al., 2013; Saal et al., 2003). Therefore, further study examining the biochemical DA metabolism between acute and chronic pain models should be conducted. We believe that our biochemistry-based data offer unique information on DA metabolism in various brain regions linked to the mesolimbic dopaminergic pathway, and on the possible mechanisms by which the changes in the level of this monoamine may shape the sensory and affective components of pain.

5. Conclusions

IMS-based visualization of monoamine neurotransmitters represents the sum of intra- and extra-cellular concentrations, most likely, the concentration of vesicular DA stored at the nerve terminals. Using this technique, we have revealed high homeostatic level of DA in the mNAc with continuous supply of *de novo* synthesized DA. Optogenetic and tactile stimulation of the sciatic nerve triggers an acute increase in DA level in the mNAc, whereas only optogenetic stimulation caused the opposite, i.e., a reduction in DA level. This study demonstrated that rapid and region-specific fluctuations in the concentration of monoamines occur in response to a sensitized, pain stimuli, and might be associated with the formation of allodynia.

Conflicts of interest

The authors declare no conflicts of interest.

Acknowledgements

This work was supported by JSPS KAKENHI, Grant Number 16H06145 (to Y.S), AMED Grant Numbers JP18gm0710012 (to Y.S.), JP18dm030727 (to Y.S. and E.S.), and the Takeda Science Foundation (to E.S.). Infrastructures of imaging MS was supported by JST ERATO Suematsu Gas Biology Project.

Appendix A. Supplementary data

Supplementary data to this article can be found online at https://doi.org/10.1016/j.neuint.2019.104494.

References

Britt, J.P., Benaliouad, F., McDevitt, R.A., Stuber, G.D., Wise, R.A., Bonci, A., 2012. Synaptic and behavioral profile of multiple glutamatergic inputs to the nucleus accumbens. Neuron 76, 790–803. https://doi.org/10.1016/j.neuron.2012.09.040.

Bromberg-Martin, E.S., Matsumoto, M., Hikosaka, O., 2010. Dopamine in motivational control: rewarding, aversive, and alerting. Neuron 68, 815–834. https://doi.org/10.1016/j.neuron.2010.11.022.

Danjo, T., Yoshimi, K., Funabiki, K., Yawata, S., Nakanishi, S., 2014. Aversive behavior induced by optogenetic inactivation of ventral tegmental area dopamine neurons is mediated by dopamine D2 receptors in the nucleus accumbens. Proc. Natl. Acad. Sci. Unit. States Am. 111, 6455–6460. https://doi.org/10.1073/pnas.1404323111.

Fibiger, H.C., McGeer, E.G., Atmadja, S., 1973. Axoplasmic transport of dopamine in nigro-striatal neurons. J. Neurochem. 21, 373–385. https://doi.org/10.1111/j.1471-4159.1973.tb04257.x.

Graziane, N.M., Polter, A.M., Briand, L.A., Pierce, R.C., Kauer, J.A., 2013. Kappa opioid receptors regulate stress-induced cocaine seeking and synaptic plasticity. Neuron 77, 942–954. https://doi.org/10.1016/j.neuron.2012.12.034.

Holly, E.N., Miczek, K.A., 2016. Ventral tegmental area dopamine revisited: effects of acute and repeated stress. Psychopharmacology (Berlin) 233, 163–186. https://doi.org/10.1007/s00213-015-4151-3.

Ikemoto, S., 2007. Dopamine reward circuitry: two projection systems from the ventral midbrain to the nucleus accumbens-olfactory tubercle complex. Brain Res. Rev. 56, 27–78. https://doi.org/10.1016/j.brainresrev.2007.05.004.

Iyer, S.M., Montgomery, K.L., Towne, C., Lee, S.Y., Ramakrishnan, C., Deisseroth, K., Delp, S.L., 2014. Virally mediated optogenetic excitation and inhibition of pain in freely moving nontransgenic mice. Nat. Biotechnol. 32, 274–278. https://doi.org/10.1038/nbt.2834.

Kai-Kai, M.A., 1984. Ultrastructural localization of [3H]dopamine in neurons of leech (Haemopis sanguisuga) abdominal ganglia. Comp. Biochem. Physiol. Part C, Comp. 78, 363–367. https://doi.org/10.1016/0742-8413(84)90099-9.

Karoum, F., Korpi, E.R., Linnoila, M., Chuang, L.W., Wyatt, R.J., 1984. Reduced metabolism and turnover rates of rat brain dopamine, norepinephrine and serotonin by chronic desipramine and zimelidine treatments. Eur. J. Pharmacol. 100, 137–144. https://doi.org/10.1016/0014-2999(84)90215-2.

Kato, T., Ide, S., Minami, M., 2016. Pain relief induces dopamine release in the rat nucleus accumbens during the early but not late phase of neuropathic pain. Neurosci. Lett. 629, 73–78. https://doi.org/10.1016/j.neulet.2016.06.060.

Kilts, C.D., Anderson, C.M., 1987. Mesoamygdaloid dopamine neurons: differential rates of dopamine turnover in discrete amygdaloid nuclei of the rat brain. Brain Res. 416, 402–408. https://doi.org/10.1016/0006-8993(87)90926-7.

Mikhailova, M.A., Deal, A.L., Grinevich, V.P., Bonin, K.D., Gainetdinov, R.R., Budygin, E.A., 2019. Real-time accumbal dopamine response to negative stimuli: effects of ethanol. ACS Chem. Neurosci. 10, 1986–1991. https://doi.org/10.1021/acschemneuro.8b00272.

Morikawa, T., Kajimura, M., Nakamura, T., Hishiki, T., Nakanishi, T., Yukutake, Y., Nagahata, Y., Ishikawa, M., Hattori, K., Takenouchi, T., Takahashi, T., Ishii, I., Matsubara, K., Kabe, Y., Uchiyama, S., Nagata, E., Gadalla, M.M., Snyder, S.H., Suematsu, M., 2012. Hypoxic regulation of the cerebral microcirculation is mediated by a carbon monoxide-sensitive hydrogen sulfide pathway. Proc. Natl. Acad. Sci. Unit. States Am. 109, 1293–1298. https://doi.org/10.1073/pnas.1119658109.

Moriya, S., Yamashita, A., Kawashima, S., Nishi, R., Yamanaka, A., Kuwaki, T., 2018. Acute aversive stimuli rapidly increase the activity of ventral tegmental area dopamine neurons in awake mice. Neuroscience 386, 16–23. https://doi.org/10.1016/j.neuroscience.2018.06.027.

Navratilova, E., Atcherley, C.W., Porreca, F., 2015. Brain circuits encoding reward from pain relief. Trends Neurosci. 38, 741–750. https://doi.org/10.1016/j.tins.2015.09.003.

Ortiz, A.N., Kurth, B.J., Osterhaus, G.L., Johnson, M.A., 2010. Dysregulation of intracellular dopamine stores revealed in the R6/2 mouse striatum. J. Neurochem. 112, 755–761. https://doi.org/10.1111/j.1471-4159.2009.06501.x.

Ren, W., Centeno, M.V., Berger, S., Wu, Y., Na, X., Liu, X., Kondapalli, J., Apkarian, A.V., Martina, M., Surmeier, D.J., 2016. The indirect pathway of the nucleus accumbens shell amplifies neuropathic pain. Nat. Neurosci. 19, 220–222. https://doi.org/10.1038/nn.4199.

Saal, D., Dong, Y., Bonci, A., Malenka, R.C., 2003. Drugs of abuse and stress trigger a common synaptic adaptation in dopamine neurons. Neuron 37, 577–582. https://doi.org/10.1016/S0896-6273(03)00021-7.

Sarkis, R., Saadé, N., Atweh, S., Jabbur, S., Al-Amin, H., 2011. Chronic dizocilpine or apomorphine and development of neuropathy in two rat models I: behavioral effects and role of nucleus accumbens. Exp. Neurol. 228, 19–29. https://doi.org/10.1016/j.expneurol.2010.12.004.

Shariatgorji, M., Nilsson, A., Goodwin, R.J.A., Källback, P., Schintu, N., Zhang, X., Crossman, A.R., Bezard, E., Svenningsson, P., Andren, P.E., 2014. Direct targeted quantitative molecular imaging of neurotransmitters in brain tissue sections. Neuron 84, 697–707. https://doi.org/10.1016/j.neuron.2014.10.011.

Szczypka, M.S., Kwok, K., Brot, M.D., Marck, B.T., Matsumoto, A.M., Donahue, B.A., Palmiter, R.D., 2001. Dopamine production in the caudate putamen restores feeding in dopamine-deficient mice. Neuron 30, 819–828. https://doi.org/10.1016/S0896-6273(01)00319-1.

Taylor, A.M.W., Becker, S., Schweinhardt, P., Cahill, C., 2016. Mesolimbic dopamine signaling in acute and chronic pain: implications for motivation, analgesia, and addiction. Pain 157, 1194–1198. https://doi.org/10.1097/j.pain.0000000000000494.

Ungless, M.A., Magill, P.J., Bolam, J.P., 2004. Uniform inhibition of dopamine neurons in the ventral tegmental area by aversive stimuli. 80. Science 303, 2040–2042. https://doi.org/10.1126/science.1093360.

Watanabe, M., Narita, Michiko, Hamada, Y., Yamashita, A., Tamura, H., Ikegami, D., Kondo, T., Shinzato, T., Shimizu, T., Fukuchi, Y., Muto, A., Okano, H., Yamanaka, A., Tawfik, V.L., Kuzumaki, N., Navratilova, E., Porreca, F., Narita, Minoru, 2018a. Activation of ventral tegmental area dopaminergic neurons reverses pathological allodynia resulting from nerve injury or bone cancer. Mol. Pain 14, 2–4. https://doi.org/10.1177/1744806918756406.

Watanabe, M., Sugiura, Y., Sugiyama, E., Narita, Michiko, Navratilova, E., Kondo, T., Uchiyama, N., Yamanaka, A., Kuzumaki, N., Porreca, F., Narita, Minoru, 2018b. Extracellular N-acetylaspartylglutamate released in the nucleus accumbens modulates the pain sensation: analysis using a microdialysis/mass spectrometry integrated system. Mol. Pain 14 174480691875493. https://doi.org/10.1177/1744806918754934.